ChemComm

COMMUNICATION

View Article Online
View Journal

Cite this: DOI: 10.1039/d6cc02368a

Received 17th April 2026,
Accepted 9th May 2026

DOI: 10.1039/d6cc02368a

rsc.li/chemcomm

Something germane about germanium: facile access to Ge_{10} adamantane

Sebastian Karger, [a] Elias Drösemeier, [b] Alexander V. Virovets, [a] Eugenia Peresypkina, [a] Hans-Wolfram Lerner, [a] Thomas Müller *[b] and Matthias Wagner *[a]

The all-germanium adamantane $(Me_3SiGe)_4(GeMe_2)_6$ (2) was synthesized from its isomer $(Me_3GeSi)_4(GeMe_2)_6$ (1) *via* sila-Wagner-Meerwein rearrangement (overall four steps starting from commercial Me_2GeCl_2, Si_2Cl_6, and $[nBu_4N]Cl$). The molecular structures of 1 and 2 were characterized by single-crystal X-ray diffraction; a plausible mechanistic scenario is postulated based on quantum-chemical calculations.

Derivatives of the rigid, cage-like hydrocarbon adamantane have found widespread applications in medicinal chemistry, functional polymers, and nanostructured materials.[1–7] Key attributes include adamantane's pronounced lipophilicity,[6] exceptional chemical inertness,[8] and well-defined three-dimensional substitution pattern.[9] Although adamantane was first isolated from crude oil in 1933[10] the systematic exploitation of its properties remained dormant for decades. It was not until Schleyer's 1957 report of a scalable synthesis *via* the $AlCl_3$-mediated skeletal rearrangement of tetrahydrodicyclopentadiene that the field expanded significantly, demonstrating that progress is inherently tied to synthetic accessibility.[11,12]

A similar bottleneck still hinders the exploration of heavier adamantane homologues. While Marschner's synthesis of the tetrasilylated Si_{10} adamantane **A** $[(Me_3SiSi)_4(SiMe_2)_6$; Fig. 1) was conceptually inspired by Schleyer's approach, it highlights the disparity between the two systems:[13] tetrahydrodicyclopentadiene is readily available through hydrogenation of dicyclopentadiene, whereas the preparation of the respective Si_{14}-precursor required elaborate oligosilane chemistry.[14] Ultimately, the synthesis of **A** long remained a labor-intensive, 10-step sequence from commercial reactants, proceeding with an overall yield below 4%.[13] The resulting limitations were in part alleviated by Su *et al.*, who optimized the Marschner protocol, thereby rendering **A** accessible in 8 steps with an overall yield of 20%.[15] This advance subsequently enabled the regioselective derivatization of **A**, as well as more comprehensive insight into its optoelectronic properties. Looking ahead, functionalized all-silicon adamantanes now provide previously missing links for systematically probing how fundamental physical features evolve during the transition from discrete molecular silicon species to silicon nanocrystals and, ultimately, the extended semiconductor lattice.[16,17]

Analogous model systems for $Si_{1-n}Ge_n$ and $Si_{1-n}Sn_n$ alloys are no less essential, given that these materials, despite their considerable application potential,[18–29] remain far less well-understood than bulk silicon. Since 2021, our groups have reported the first mixed Si_xGe_y and Si_xSn_y adamantanes.[26,29] A distinct advantage over **A** is that these compounds can be accessed in one-pot reactions of Me_2GeCl_2 or Me_2SnCl_2 with $[SiCl_3]^-$, generated *in situ via* chloride-induced heterolysis of Si_2Cl_6.[30–32] As a representative example, the Si_4Ge_6 adamantane **B** was obtained in 40–45% yield (Fig. 1); likewise, analogues with Si_5Ge_5, Si_6Ge_4, Si_5Sn_5, and Si_6Sn_4 skeletal compositions and Ge/Sn atoms occupying the secondary (2°) core positions were isolated in pure form. Later, we disclosed the synthesis of compound **C**, which contains four Ge atoms in quaternary (4°) positions, *via* sila-Wagner–Meerwein rearrangement[33–42] of the permethylated Si_6Ge_4 adamantane **D** (Scheme 1).[43] Parallel to this research, Su *et al.* obtained the same

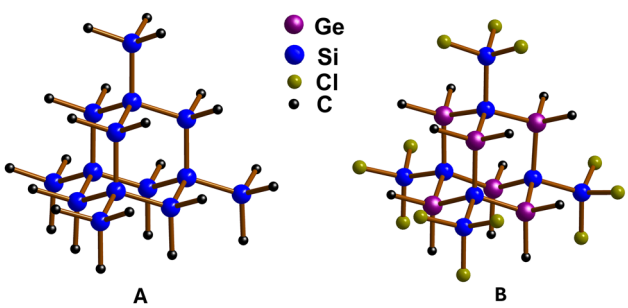

Fig. 1 Solid-state structures of the Si_{10} adamantane **A** and the Si_4Ge_6 adamantane **B**.

[a] Institute of Inorganic and Analytical Chemistry, Goethe University Frankfurt, Max-von-Laue-Straße 7, Frankfurt am Main, 60438, Germany. E-mail: matthias.wagner@chemie.uni-frankfurt.de
[b] Institute of Chemistry, Carl von Ossietzky Universität Oldenburg, Carl von Ossietzky-Str. 9-11, Oldenburg, 26129, Germany. E-mail: thomas.mueller@uni-oldenburg.de

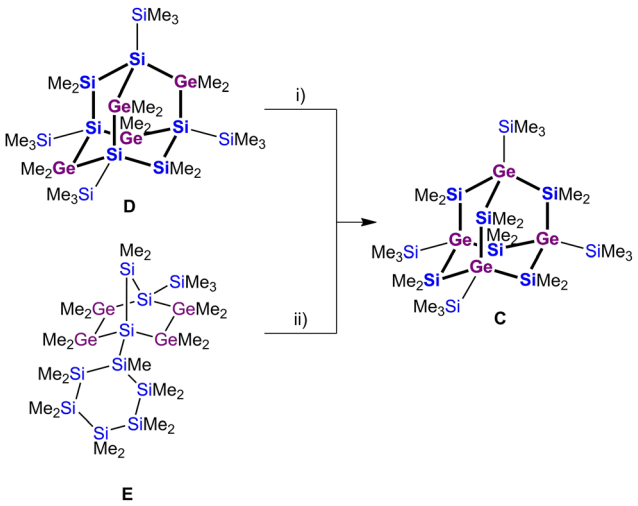

Scheme 1 Synthesis of the Si_6Ge_4 adamantane **C** *via* skeletal rearrangements of the precursors **D** or **E**. (i) 0.1 equiv. $[Ph_3C][B(C_6F_5)_4]$, toluene, r.t., 2 d, 69% yield; (ii) 0.2 equiv. $[Ph_3C][B(C_6F_5)_4]$, CH_2Cl_2, r.t., 2 d, 65% yield.

compound through Lewis acid-mediated rearrangement of the mixed Si/Ge precursor **E** in a demanding multistep sequence (Scheme 1).[44]

A logical next synthetic target is the hitherto unknown Ge_{10} adamantane. This is not only because it constitutes the unit cell of stable cubic α-germanium, but also because it would provide the first heteroadamantane containing Ge–Ge bonds. Herein, we demonstrate that this compound is indeed accessible *via* a three-step sequence, building on the insights into group 14 heteroadamantanes outlined above: in the first step, **B** is permethylated, followed by a fourfold Me_3Si/Me_3Ge exchange and, finally, migration of the four peripheral Ge atoms into the cluster core through a sila-Wagner–Meerwein rearrangement (Scheme 2a).

The synthesis of the crucial Si_4Ge_6 precursor $\mathbf{B^{TMS}}$ (TMS: Me_3Si) was accomplished on a 200 mg scale through permethylation of **B** with an excess of MeMgBr in THF/Et_2O according to a published room-temperature protocol.[29] For the installation of the four Me_3Ge substituents, we relied on Marschner's[45–47] KO*t*Bu-induced Si–Si bond-cleavage reaction. Specifically, a mixture of $\mathbf{B^{TMS}}$ and KO*t*Bu/18-crown-6 (6 equiv.) in THF was treated slowly and dropwise with a THF solution of Me_3GeCl (8 equiv.) at ambient temperature. Workup afforded the fourfold germylated Si_4Ge_6 adamantane **1** in 59% yield. We note that employing the formally required stoichiometry of 1 : 4 : 4 : 4 (rather than the actually employed 1 : 6 : 6 : 8 ratio) led to a less selective conversion. The skeletal-editing transformation to furnish the targeted all-germanium adamantane **2** was performed in toluene at 60 °C over 4 d (sealed glass ampoule). $[Ph_3C][B(C_6F_5)_4]$ (0.1 equiv.) served as the Lewis-acidic catalyst (87% yield). For a successful rearrangement step, it is crucial to completely remove the crown ether prior to the reaction by chromatographic purification. Crystals of $\mathbf{1}\cdot 0.75(C_5H_{12})$ and $\mathbf{2}\cdot 0.75(C_5H_{12})$ suitable for X-ray diffraction (SCXRD) were grown from their *n*-pentane solutions by slow evaporation. The facile conversion $\mathbf{B^{TMS}} \rightarrow \mathbf{1}$ is particularly remarkable in light of the observation by Su *et al.* that an analogous Me_3Si/Me_3Ge exchange on the Si_{10} adamantane **A** can be carried out at most twice, which "limits the efficiency of accessing SiGe adamantanes with >2 Ge atoms *via* skeletal editing if starting from **A**".[44] We assume that, in the present case, the specific reaction conditions promote a sequential substitution of all four Me_3Si groups, although the number of silanide vertices coexisting on the same heteroadamantane intermediate remains unknown. The very formation of silanide intermediates was demonstrated by reaction of $\mathbf{B^{TMS}}$ with 1 equiv. of KO*t*Bu/18-crown-6 in THF-d_8: NMR spectroscopic analysis unambiguously indicated the essentially quantitative conversion to the monosilanide $[\mathbf{3}]^-$ (Scheme 2b). After solvent exchange to C_6H_6, the salt [K(18-c-6)][**3**] was isolated in crystalline form and characterized by SCXRD.

While $\mathbf{B^{TMS}}$ gives rise to two distinct ^{29}Si NMR signals at −3.9 (Me_3Si) and −97.7 ppm (4° Si), only a single resonance is detectable for each of the compounds **1** (−88.8 ppm; 4° Si) and **2** (1.4 ppm; Me_3Si). The replacement of Me_3Si by the more electronegative Me_3Ge group upon going from $\mathbf{B^{TMS}}$ to **1** is thus accompanied by a deshielding of the corresponding Si vertex by 9 ppm; a comparable deshielding has been reported for the all-silicon adamantane **A** (−118.6 ppm)[13] after exchange of one of its Me_3Si substituents for a Me_3Ge group (−110.7 ppm).[15] Furthermore, the experimentally determined $\delta(^{29}Si)$ chemical shifts of **1** and **2** are in good agreement with the computed

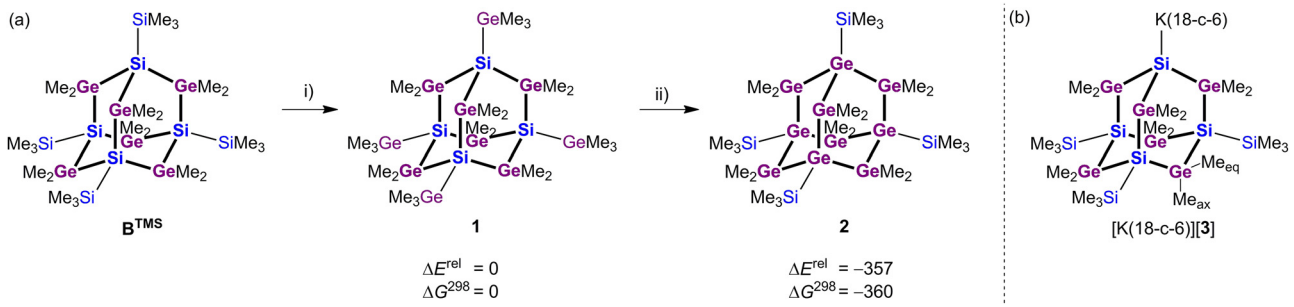

Scheme 2 (a) Synthesis of the Ge_{10} adamantane **2**, starting from $\mathbf{B^{TMS}}$ and proceeding *via* **1**; computed relative energies ΔE^{rel}/Gibbs free enthalpies ΔG^{298} in kJ mol^{-1} for the isomers **1** and **2** are also provided (MN15/def2-TZVP). (i) 6 equiv. KO*t*Bu, 6 equiv. 18-crown-6, 8 equiv. Me_3GeCl, THF, r.t., 20 min, 59% yield; (ii) 0.1 equiv. $[Ph_3C][B(C_6F_5)_4]$, toluene, 60 °C, 4 d, 87% yield. (b) Structural motif of the silanide [K(18-c-6)][**3**].

values (Table S6). Each of the compounds $\mathbf{B}^{\mathbf{TMS}}$, **1**, and **2** displays only two ^{1}H and two ^{13}C NMR resonances, consistent with their proposed T_d-symmetric molecular frameworks. Symmetry breaking due to the absence of one Me_3Si substituent in the monosilanide $[\mathbf{3}]^-$ results in four distinct ^{1}H NMR signals: one corresponds to the remaining three Me_3Si substituents (27*H*), one to the α-$GeMe_2$ units (18*H*), and two to the axial and equatorial-pointing $GeMe_{ax}$ (9*H*) and $GeMe_{eq}$ (9*H*) groups, respectively (Scheme 2b). Compared to the tetrahedrally coordinated *Si*–$SiMe_3$ vertices ($\delta(^{29}Si) = -109.4$), the resonance of the silanide site appears slightly downfield ($\delta(^{29}Si) = -96.3$).

The four Si_xGe_y adamantanes **A**, $\mathbf{B}^{\mathbf{TMS}}$, **1**, and **2** show very similar UV/vis absorption spectra with peak maxima (λ_{max}) in the range 222–228 nm (in cyclohexane; Table S1).[13] These similarities are consistent with previous studies on Si_xGe_y adamantanes[44] and nanoscale $Si_{1-n}Ge_n$ crystals,[48] indicating only a small effect of increasing Ge content on the optical band gaps.[49]

The rhombohedral unit cells of **1** and **2** each contain a single crystallographically unique molecule located on a C_3 axis that passes through one of the E–EMe_3 bonds and the center of the opposite boat-like E_6 ring (Fig. 2; E = Si, Ge). Successful Me_3Si/Me_3Ge exchange is evidenced by the fitting atomic scattering factors for the peripheral, heavy Ge atoms and by the elongated average Si–EMe_3 bond length in **1** (2.399[3] Å; E = Ge) compared to $\mathbf{B}^{\mathbf{TMS}}$ (2.3567[7] Å; E = Si; *cf.* **FEWWAJ** = $\mathbf{B}^{\mathbf{TMS}}$ in Table S11);[29] the corresponding average Ge–$SiMe_3$ bond length in **2** is 2.396[2] Å.[50] As expected, the average Ge–Ge bond length within the cluster core of the Ge_{10} adamantane **2** is further increased to 2.433[1] Å, in good agreement with representative literature values.[39,50–52] [K(18-c-6)][**3**] forms C_s-symmetric contact-ion pairs in the solid state ($K^+\cdots Si^-$ = 3.388(2) Å; Fig. 2). The sum of the Ge–Si–Ge bond angles at the silanide center of $[\mathbf{3}]^-$ amounts to 304.5(2)°, which is significantly smaller than the corresponding average value of 324.1(2)° for the tetrahedral *Si*–$SiMe_3$ centers. The higher degree of pyramidalization of the silanide vertex indicates pronounced *s*-character of the electron lone pair and a corresponding increase in p-orbital contribution to the Si–Ge bonds, in agreement with Bent's rule.[53]

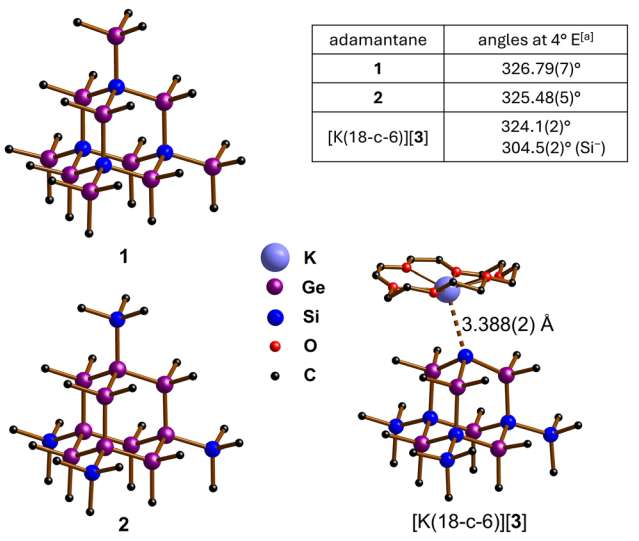

adamantane	angles at 4° E[a]
1	326.79(7)°
2	325.48(5)°
[K(18-c-6)][**3**]	324.1(2)° 304.5(2)° (Si^-)

Fig. 2 Molecular structures of **1**, **2**, and contact-ion pair [K(18-c-6)][**3**] in the solid state; H atoms are omitted for clarity. Average angle sums at the quaternary E vertices (4° E) are given in the Table. [a] E = Si, Ge; see the SI for more details.

Density functional theory (DFT) calculations at the MN15/def2-TZVP level (see the SI for details) indicate that the isomerization of the germylated Si_4Ge_6 adamantane **1** to the silylated Ge_{10} adamantane **2** is exothermic by 357 kJ mol^{-1} (Scheme 2a and SI). A conceivable Si_4Ge_6 adamantane isomer featuring all four Si atoms in 2° positions, lies energetically between isomers **1** and **2** (*cf.* **F**; Fig. S19). The selective formation of isomer **2** suggests that the sila-Wagner-Meerwein rearrangement of these clusters is thermodynamically controlled.[43] In particular, the resulting greater number of Si–C bonds, combined with their higher bond dissociation energy (BDE = 385 kJ mol^{-1}) relative to the Ge–C bond (332 kJ mol^{-1}), outcompetes the energetic penalty of replacing stronger Ge–Si (311 kJ mol^{-1}) with weaker Ge–Ge bonds (293 kJ mol^{-1}; see Table S3 for calculated BDEs). Specifically, the **1** → **2** conversion is associated with the exchange of twelve Ge–C bonds for twelve stronger Si–C bonds ($\Delta(\Sigma BDE) = -636$ kJ mol^{-1}) and of twelve Si–Ge bonds by twelve weaker Ge–Ge bonds ($\Delta(\Sigma BDE) = 216$ kJ mol^{-1}). A simple additive estimate based on these increments yields an overall energy difference of −420 kJ mol^{-1} in favor of **2**, which is close to the DFT-computed energy difference between **1** and **2** of −357 kJ mol^{-1} (Scheme 2a).

We investigated the $[Ph_3C]^+$-catalyzed isomerization **1** → **2** in detail. Previous experimental and computational studies on related systems have shown that the initial step in this type of reaction involves the formation of silylium or germylium ions *via* Me^--anion transfer from the Si_xGe_y oligomer to the $[Ph_3C]^+$ cation.[54] Following rearrangement to the thermodynamically most stable silylium or germylium ion, this species finally abstracts Me^- from another molecule of the starting material (here **1**), thereby affording the product and initiating the next rearrangement event. Me^- abstraction from **1** leads to two possible cations, $[\mathbf{G}]^+$ and $[\mathbf{H}]^+$, with the 2° germylium ion $[\mathbf{G}]^+$ being more stable by 16 kJ mol^{-1} than the *exo*-cluster germylium ion $[\mathbf{H}]^+$ (Scheme 3a). Both $[\mathbf{G}]^+$ and $[\mathbf{H}]^+$ are significantly higher in energy than the cations $[\mathbf{I}]^+$ and $[\mathbf{J}]^+$, which are plausible immediate precursors of the final product **2**. The enhanced stability of $[\mathbf{I}]^+$ and $[\mathbf{J}]^+$ arises from the *exo*-cage position of all four Si atoms, thus maximizing the number of strong Si–C bonds. Consequently, the isomerization of the 2° germylium ions $[\mathbf{G}]^+$ → $[\mathbf{I}]^+$ corresponds to the most exothermic rearrangement pathway (−371 kJ mol^{-1}; Scheme 3a).

The large exothermicity of the transformation $[\mathbf{G}]^+$ → $[\mathbf{I}]^+$ guarantees the catalytic nature of the reaction although the regeneration of germylium ion $[\mathbf{G}]^+$ by Me^- transfer from the Si_4Ge_6 adamantane **1** to $[\mathbf{I}]^+$ is slightly endergonic (ΔG^R = +15 kJ mol^{-1}, Scheme 3b).

While bulk silicon and germanium remain foundational semiconductor materials, the drive toward device miniaturization necessitates a deeper understanding of how quantum confinement reshapes their physical properties at the nanoscale.[55,56] In contrast to the extensive body of work on silicon nanoclusters,[57–60] their germanium counterparts are still comparatively underexplored[61–65] – notwithstanding the current renaissance of germanium in

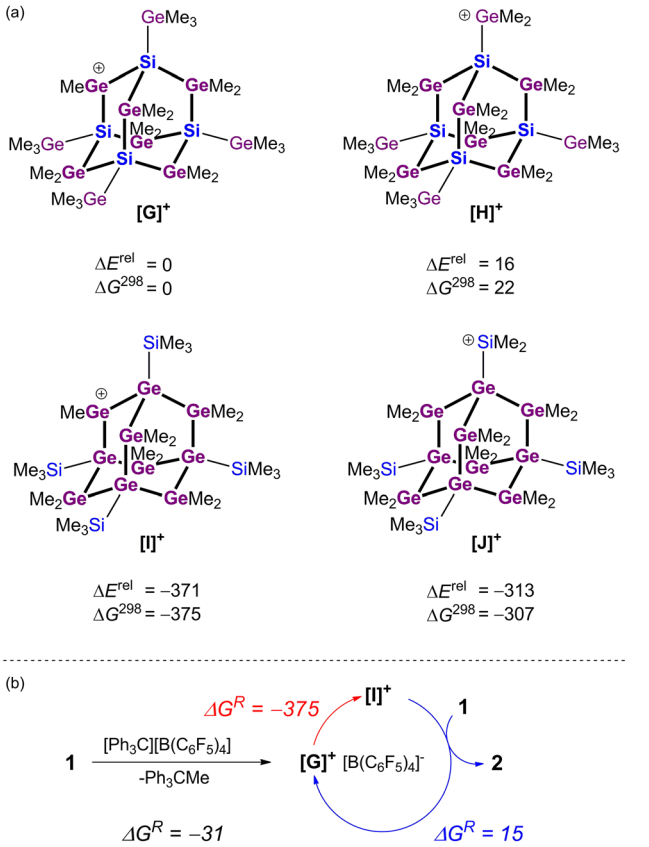

Scheme 3 (a) Relative energies ΔE^{rel} and Gibbs free enthalpies ΔG^{298} of cations derived from **1** ($[\mathbf{G}]^+$, $[\mathbf{H}]^+$) and **2** ($[\mathbf{I}]^+$, $[\mathbf{J}]^+$) in kJ mol^{-1} (MN15/def2-TZVP). (b) Catalytic cycle for the isomerization of the Si_4Ge_6 adamantane **1** to **2**, initiated by $[Ph_3C][B(C_6F_5)_4]$. Gibbs free reaction enthalpies ΔG^R are given in kJ mol^{-1} in italics (MN15/def2-TZVP).

optoelectronic applications. Currently, the field of molecular germanium clusters is dominated by soluble polyhedral Zintl anions and unsaturated metalloid species.[65,66] Prominent examples are the *nido*-cluster $[Ge_9]^{4-}$ (Corbett)[67] and its silylated derivative $[Ge_9(Si(SiMe_3)_3)_3]^-$ (Schnepf, Sevov).[68,69] These clusters contain both 'naked' and substituent-bound Ge atoms. In contrast, **2** bears a peripheral group at each Ge atom and is thus an electron-precise saturated cage paralleled only by the tetragermatetrahedrane $[Ge(SitBu_3)]_4$,[70] hexagermaprismane $[Ge(CH(SiMe_3)_2)]_6$,[71] and octagermacubane $[Ge(CMeEt_2)]_8$.[72] Unlike these smaller polyhedral species, the Ge_{10} adamantane **2** is free of strain and represents the fundamental structural motif of α-germanium. Given conflicting theoretical reports[73] regarding the extent of σ-delocalization[74,75] and quantum-confinement effects in all-tetrel adamantanes and diamantanes, the scalable synthesis and foreseeable rich derivatization chemistry of **2** will enable the critical validation of existing theoretical models through robust experimental data.

Author contributions

S. K. performed all experimental studies and characterized the new compounds. E. D. carried out the quantum-chemical calculations. A. V. V. and E. P. performed the X-ray crystal structure analyses of all compounds. H.-W. L., T. M., and M. W. supervised the project. The manuscript was written by S. K., T. M., and M. W. and edited by all co-authors.

Conflicts of interest

There are no conflicts of interest.

Data availability

Data supporting the findings of this study are available within the supplementary information (SI). Supplementary information: synthetic procedures, NMR spectra, photophysical data, X-ray crystallographic data, and computational details. See DOI: https://doi.org/10.1039/d6cc02368a.

CCDC 2545827–2545829 contain the supplementary crystallographic data for this paper.[76a–c]

Acknowledgements

This work was supported by the Deutsche Forschungsgemeinschaft (DFG, MU1440/16-1 and WA 864/9-1, project 544135113). The authors are grateful to Evonik Resource Efficiency GmbH, Rheinfelden (Germany), for the generous donation of $GeCl_4$ and Si_2Cl_6. Parts of this research were carried out on the P24 beamline (project R-20250872) at PETRA III at DESY, a member of the Helmholtz Association (HGF). We thank Dr M. Tolkiehn for his assistance with the use of beamline P24. Computations were done at the HPC Cluster ROSA at the Carl von Ossietzky University of Oldenburg, funded by the DFG (INST 184/225-1 FUGG) and the Ministry of Science and Culture (MWK) of the Lower Saxony State.

References

1 G. R. Newkome, A. Nayak, R. K. Behera, C. N. Moorefield and G. R. Baker, *J. Org. Chem.*, 1992, **57**, 358–362.
2 B. Chen, M. Eddaoudi, T. M. Reineke, J. W. Kampf, M. O'Keeffe and O. M. Yaghi, *J. Am. Chem. Soc.*, 2000, **122**, 11559–11560.
3 S. Zheng, J. Shi and R. Mateu, *Chem. Mater.*, 2000, **12**, 1814–1817.
4 H. Ramezani and G. A. Mansoori, in *Molecular Building Blocks for Nanotechnology*, ed. G. A. Mansoori, T. F. George, L. Assoufid and G. Zhang, Springer, New York, 1st edn, 2007, pp. 44–71.
5 Y. Xue and G. A. Mansoori, *Int. J. Nanosci.*, 2008, **7**, 63–72.
6 L. Wanka, K. Iqbal and P. R. Schreiner, *Chem. Rev.*, 2013, **113**, 3516–3604.
7 K. Spilovska, F. Zemek, J. Korabecny, E. Nepovimova, O. Soukup, M. Windisch and K. Kuca, *Curr. Med. Chem.*, 2016, **23**, 3245–3266.
8 J. E. Dahl, J. M. Moldowan, K. E. Peters, G. E. Claypool, M. A. Rooney, G. E. Michael, M. R. Mello and M. L. Kohnen, *Nature*, 1999, **399**, 54–57.
9 Q. Li, A. V. Rukavishnikov, P. A. Petukhov, T. O. Zaikova, C. Jin and J. F. W. Keana, *J. Org. Chem.*, 2003, **68**, 4862–4869.
10 S. Lada and V. Macháček, *Collect. Czech. Chem. Commun.*, 1933, **5**, 1–5.
11 P. von Ragué Schleyer, *J. Am. Chem. Soc.*, 1957, **79**, 3292.
12 K. E. Wentz, A. F. Gittens and R. S. Klausen, *J. Am. Chem. Soc.*, 2025, **147**, 2938–2959.
13 J. Fischer, J. Baumgartner and C. Marschner, *Science*, 2005, **310**, 825.
14 R. Fischer, T. Konopa, S. Ully, J. Baumgartner and C. Marschner, *J. Organomet. Chem.*, 2003, **685**, 79–92.

15 T. C. Siu, M. Imex Aguirre Cardenas, J. Seo, K. Boctor, M. G. Shimono, I. T. Tran, V. Carta and T. A. Su, *Angew. Chem., Int. Ed.*, 2022, **61**, e202206877.
16 M. O. Hight and T. A. Su, *Trends Chem.*, 2024, **6**, 365–376.
17 M. O. Hight, A. E. Pimentel, T. C. Siu, J. Y. Wong, J. Nguyen, V. Carta and T. A. Su, *J. Am. Chem. Soc.*, 2025, **147**, 16602–16610.
18 S. Sedky, A. Witvrouw and K. Baert, *Sens. Actuators, A*, 2002, **97–98**, 503–511.
19 B. Mheen, Y.-J. Song, J.-Y. Kang and S. Hong, *ETRI J.*, 2005, **27**, 439–445.
20 G. L. Wang, M. Moeen, A. Abedin, M. Kolahdouz, J. Luo, C. L. Qin, H. L. Zhu, J. Yan, H. Z. Yin, J. F. Li, C. Zhao and H. H. Radamson, *J. Appl. Phys.*, 2013, **114**, 123511.
21 S. Cecchi, E. Gatti, D. Chrastina, J. Frigerio, E. Müller Gubler, D. J. Paul, M. Guzzi and G. Isella, *J. Appl. Phys.*, 2014, **115**, 093502.
22 Y. S. Li, P. Sookchoo, X. Cui, R. Mohr, D. E. Savage, R. H. Foote, R. Jacobsen, J. R. Sánchez-Pérez, D. M. Paskiewicz, X. Wu, D. R. Ward, S. N. Coppersmith, M. A. Eriksson and M. G. Lagally, *ACS Nano*, 2015, **9**, 4891–4899.
23 D. Marris-Morini, V. Vakarin, J. M. Ramirez, Q. Liu, A. Ballabio, J. Frigerio, M. Montesinos, C. Alonso-Ramos, X. Le Roux, S. Serna, D. Benedikovic, D. Chrastina, L. Vivien and G. Isella, *Nanophotonics*, 2018, **7**, 1781–1793.
24 J. Aberl, M. Brehm, T. Fromherz, J. Schuster, J. Frigerio and P. Rauter, *Opt. Express*, 2019, **27**, 32009–32018.
25 E. M. T. Fadaly, A. Dijkstra, J. R. Suckert, D. Ziss, M. A. J. van Tilburg, C. Mao, Y. Ren, V. T. van Lange, K. Korzun, S. Kölling, M. A. Verheijen, D. Busse, C. Rödl, J. Furthmüller, F. Bechstedt, J. Stangl, J. J. Finley, S. Botti, J. E. M. Haverkort and E. P. A. M. Bakkers, *Nature*, 2020, **580**, 205–209.
26 B. Köstler, M. Bolte, H.-W. Lerner and M. Wagner, *Chem. – Eur. J.*, 2021, **27**, 14401–14404.
27 B. Köstler, F. Jungwirth, L. Achenbach, M. Sistani, M. Bolte, H.-W. Lerner, P. Albert, M. Wagner and S. Barth, *Inorg. Chem.*, 2022, **61**, 17248–17255.
28 R. Behrle, V. Krause, M. S. Seifner, B. Köstler, K. A. Dick, M. Wagner, M. Sistani and S. Barth, *Nanomaterials*, 2023, **13**, 627.
29 B. Köstler, J. Gilmer, M. Bolte, A. Virovets, H.-W. Lerner, P. Albert, F. Fantuzzi and M. Wagner, *Chem. Commun.*, 2023, **59**, 2295–2298.
30 J. Tillmann, L. Meyer, J. I. Schweizer, M. Bolte, H.-W. Lerner, M. Wagner and M. C. Holthausen, *Chem. – Eur. J.*, 2014, **20**, 9234–9239.
31 J. Teichmann, M. Bursch, B. Köstler, M. Bolte, H.-W. Lerner, S. Grimme and M. Wagner, *Inorg. Chem.*, 2017, **56**, 8683–8688.
32 J. Teichmann and M. Wagner, *Chem. Commun.*, 2018, **54**, 1397–1412.
33 M. Ishikawa and M. Kumada, *J. Chem. Soc. D*, 1970, 157.
34 M. Ishikawa, J. Iyoda, H. Ikeda, K. Kotake, T. Hashimoto and M. Kumada, *J. Am. Chem. Soc.*, 1981, **103**, 4845–4850.
35 M. Ishikawa, M. Watanabe, J. Iyoda, H. Ikeda and M. Kumada, *Organometallics*, 1982, **1**, 317–322.
36 T. A. Blinka and R. West, *Organometallics*, 1986, **5**, 128–133.
37 S. Sharma, N. Caballero, H. Li and K. H. Pannell, *Organometallics*, 1999, **18**, 2855–2860.
38 H. Wagner, A. Wallner, J. Fischer, M. Flock, J. Baumgartner and C. Marschner, *Organometallics*, 2007, **26**, 6704–6717.
39 H. Wagner, J. Baumgartner, T. Müller and C. Marschner, *J. Am. Chem. Soc.*, 2009, **131**, 5022–5023.
40 L. Albers, M. A. Meshgi, J. Baumgartner, C. Marschner and T. Müller, *Organometallics*, 2015, **34**, 3756–3763.
41 L. Albers, S. Rathjen, J. Baumgartner, C. Marschner and T. Müller, *J. Am. Chem. Soc.*, 2016, **138**, 6886–6892.
42 L. Albers, J. Baumgartner, C. Marschner and T. Müller, *Chem. – Eur. J.*, 2016, **22**, 7970–7977.
43 S. Kühn, B. Köstler, C. True, L. Albers, M. Wagner, T. Müller and C. Marschner, *Chem. Sci.*, 2023, **14**, 8956–8961.
44 M. Imex Aguirre Cardenas, T. C. Siu, A. E. Pimentel, M. O. Hight, M. G. Shimono, S. Thai, V. Carta and T. A. Su, *J. Am. Chem. Soc.*, 2023, **145**, 20588–20594.
45 C. Marschner, *Eur. J. Inorg. Chem.*, 1998, 221–226.
46 C. Kayser, R. Fischer, J. Baumgartner and C. Marschner, *Organometallics*, 2002, **21**, 1023–1030.
47 R. Fischer, D. Frank, W. Gaderbauer, C. Kayser, C. Mechtler, J. Baumgartner and C. Marschner, *Organometallics*, 2003, **22**, 3723–3731.
48 X. D. Pi and U. Kortshagen, *Nanotechnology*, 2009, **20**, 295602.
49 J. E. Vincent, J. Kim and R. M. Martin, *Phys. Rev. B: Condens. Matter Mater. Phys.*, 2007, **75**, 045302.
50 Standard deviations for the averaged bond lengths, including symmetry equivalents, are given in square brackets.
51 K. D. Roewe, A. L. Rheingold and C. S. Weinert, *Chem. Commun.*, 2013, **49**, 8380–8382.
52 K. V. Zaitsev, A. A. Kapranov, A. V. Churakov, O. K. Poleshchuk, Y. F. Oprunenko, B. N. Tarasevich, G. S. Zaitseva and S. S. Karlov, *Organometallics*, 2013, **32**, 6500–6510.
53 J. P. Foster and F. Weinhold, *J. Am. Chem. Soc.*, 1980, **102**, 7211–7218.
54 T. Müller, in *Organogermanium Compounds: Theory, Experiment, and Applications*, ed. V. Y. Lee, John Wiley & Sons, Inc., Hoboken, 1st edn, 2023, pp. 299–338.
55 A. L. Efros and M. Rosen, *Annu. Rev. Mater. Sci.*, 2000, **30**, 475–521.
56 S. M. Reimann and M. Manninen, *Rev. Mod. Phys.*, 2002, **74**, 1283–1342.
57 J. Tillmann, J. H. Wender, U. Bahr, M. Bolte, H.-W. Lerner, M. C. Holthausen and M. Wagner, *Angew. Chem., Int. Ed.*, 2015, **54**, 5429–5433.
58 S. Kyushin, in *Organosilicon Compounds*, ed. V. Y. Lee, Elsevier Inc., 2017, pp. 69–144.
59 Y. Heider and D. Scheschkewitz, *Chem. Rev.*, 2021, **121**, 9674–9718.
60 M. Bamberg, M. Bursch, A. Hansen, M. Brandl, G. Sentis, L. Kunze, M. Bolte, H.-W. Lerner, S. Grimme and M. Wagner, *J. Am. Chem. Soc.*, 2021, **143**, 10865–10871.
61 M. L. Amadoruge and C. S. Weinert, *Chem. Rev.*, 2008, **108**, 4253–4294.
62 A. Schnepf, *Eur. J. Inorg. Chem.*, 2008, 1007–1018.
63 A. Schnepf, *New J. Chem.*, 2010, **34**, 2079–2092.
64 C. S. Weinert, *Comments Inorg. Chem.*, 2011, **32**, 55–87.
65 S. Scharfe, F. Kraus, S. Stegmaier, A. Schier and T. F. Fässler, *Angew. Chem., Int. Ed.*, 2011, **50**, 3630–3670.
66 T. Kunz and A. Schnepf, in *Organogermanium Compounds: Theory, Experiment, and Applications*, ed. V. Y. Lee, John Wiley & Sons, Inc., Hoboken, 1st edn, 2023, pp. 225–275.
67 C. E. Belin, J. D. Corbett and A. Cisar, *J. Am. Chem. Soc.*, 1977, **99**, 7163–7169.
68 A. Schnepf, *Angew. Chem., Int. Ed.*, 2003, **42**, 2624–2625.
69 F. Li and S. C. Sevov, *Inorg. Chem.*, 2012, **51**, 2706–2708.
70 N. Wiberg, W. Hochmuth, H. Nöth, A. Appel and M. Schmidt-Amelunxen, *Angew. Chem., Int. Ed. Engl.*, 1996, **35**, 1333–1334.
71 A. Sekiguchi, C. Kabuto and H. Sakurai, *Angew. Chem., Int. Ed. Engl.*, 1989, **28**, 55–56.
72 A. Sekiguchi, T. Yatabe, H. Kamatani, C. Kabuto and H. Sakurai, *J. Am. Chem. Soc.*, 1992, **114**, 6260–6262.
73 F. Marsusi, K. Mirabbaszadeh and G. A. Mansoori, *Phys. E*, 2009, **41**, 1151–1156.
74 R. D. Miller, *Chem. Rev.*, 1989, **89**, 1359–1410.
75 J. Hlina, R. Zitz, H. Wagner, F. Stella, J. Baumgartner and C. Marschner, *Inorg. Chim. Acta*, 2014, **422**, 120–133.
76 (*a*) CCDC 2545827: Experimental Crystal Structure Determination, 2026, DOI: 10.5517/ccdc.csd.cc2rg4gv; (*b*) CCDC 2545828: Experimental Crystal Structure Determination, 2026, DOI: 10.5517/ccdc.csd.cc2rg4hw; (*c*) CCDC 2545829: Experimental Crystal Structure Determination, 2026, DOI: 10.5517/ccdc.csd.cc2rg4jx.